

9840

NACA TN 3553

NATIONAL ADVISORY COMMITTEE FOR AERONAUTICS

TECHNICAL NOTE 3553

COMPRESSIVE CRIPPLING OF STRUCTURAL SECTIONS

By Melvin S. Anderson

Langley Aeronautical Laboratory
Langley Field, Va.



Washington

January 1956

0066674



TECH LIBRARY KAFB, NM

AFMDC
TECHNICAL LIBRARY
AFMDC



TECHNICAL NOTE 3553

COMPRESSIVE CRIPPLING OF STRUCTURAL SECTIONS

By Melvin S. Anderson

SUMMARY

A method is presented for calculating crippling stresses of structural sections as a function of material properties and the proportions of the section. The presence of formed or anisotropic material is accounted for by the use of an effective stress-strain curve. The method of analysis applies to many sections for which a procedure for calculating crippling stresses was not previously available.

INTRODUCTION

An important part of structural design is the determination of allowable compressive loads for the columns and stiffeners of the basic aircraft structure. If a member, such as a long column, is not subject to local buckling, the maximum load can be adequately predicted by Euler's column formula with the tangent modulus used for inelastic stresses. However, for shorter lengths, many sections composed of plate elements buckle locally before the column load is reached, causing a reduction in column stiffness and a corresponding reduction in the ultimate load. As length is decreased, a point is reached where failure is primarily a function of the cross-sectional proportions. For this portion of the column curve, strength is relatively independent of length, and the average stress at maximum load has been referred to as the crippling stress. For practical purposes, then, the crippling stress is the highest stress that can be achieved by a section and provides an index to the capacity of the section to carry compressive load.

Because the essentially exact determination of crippling stresses is extremely difficult, information necessary for design has been obtained experimentally by testing various sections representative of the shapes, proportions, and materials in current use. This approach is adequate if one does not have to consider many materials or a wide variation in the properties of the material. However, the temperatures achieved in high-speed flight require the introduction of heat-resistant materials and consideration of the effects of temperature on material properties. The experimental determination of crippling

stresses under these conditions tends to become unwieldy. In order to eliminate the need for extensive testing programs, several investigators have developed empirical crippling-strength equations, based on the available data, relating crippling stress to the proportions of a section and the properties of the material. In reference 1, a method is presented for predicting the crippling strength of formed channel and Z-sections and extruded channel, Z-, and H-sections having webs with relatively small width-thickness ratios. Tests made in the present investigation indicate that the equations presented in reference 1 cannot be extended to sections for which the width of the web is large with respect to its thickness, and therefore probably cannot be considered to apply to extrusions in general. In reference 2 a method is presented that will apply to any formed section, but such an analysis has not been made for extruded sections. The purpose of the present paper is to introduce a method of predicting crippling stresses which will include the range already considered as well as sections for which a method was not previously available.

Much of the material presented in this report was submitted to the Virginia Polytechnic Institute as a thesis in partial fulfillment of the requirements for the degree of Master of Science in Applied Mechanics.

SYMBOLS

a	length of plate element
A	cross-sectional area of plate element
b	width of plate element
b'	developed width of a section
C, K, n	constants
D	plate flexural stiffness per unit width, $\frac{Et^3}{12(1 - \mu^2)}$
E	modulus of elasticity
E _s	secant modulus
E _t	tangent modulus
E _s '	secant modulus at σ_n when $\bar{\sigma} \leq \sigma_n$; secant modulus at $\bar{\sigma}$ when $\bar{\sigma} > \sigma_n$

I	moment of inertia
k	buckling-stress coefficient
m	ratio of initial slope, after elastic buckling, of curve of average stress plotted against unit shortening to slope of material stress-strain curve
p	integer corresponding to number of buckles in a plate
P	load
t	thickness of plate element
ϵ	strain
ϵ_{cr}	buckling strain
ϵ_e	unit shortening
ϵ_n	strain at which $E_t = \frac{1}{n} E_s$
η	plasticity reduction factor

$$\theta = \frac{EI_F}{b_W D_W} - \frac{A_F \sigma_{cr} a^2}{b_W D_W p^2 \pi^2}$$

μ	Poisson's ratio
σ	stress
$\bar{\sigma}$	average stress
σ_{cr}	buckling stress
σ_{el}	elastic buckling stress
$\bar{\sigma}_f$	crippling stress of a section
σ_e	average edge stress corresponding to strain ϵ_e
σ_{cy}	0.2-percent-offset compressive yield stress
σ_n	stress at which $E_t = \frac{1}{n} E_s$

Subscripts:

F	flange
S	skin of a sheet-stringer panel
W	web
max	maximum

ANALYSIS

Crippling failures can be divided into two categories: one in which local buckling is initiated in the high-stress region (stresses greater than about three-fourths of the yield stress) with failure occurring at little or no increase in load, and one in which local buckling is elastic with a definite margin between buckling and maximum load. Calculation of the crippling stress for the first case is in essence a calculation of the plastic buckling stress. A convenient procedure for computing plastic buckling stresses is to relate the stress at which buckling would occur if the material were perfectly elastic to the actual buckling stress by means of a plasticity reduction factor η which is a function of the stress level. A value of η that is simple to compute and correlates with test data is $\sqrt{E_t/E}$. The buckling stress is then given by

$$\sigma_{cr} = \eta \sigma_{e\lambda} \quad (1)$$

where

$$\eta = \sqrt{E_t/E}$$

The problem that remains, then, is the calculation of the crippling stress of sections which buckle elastically and then sustain further load before failure.

One of the earliest methods used for predicting crippling stresses was to calculate the buckling stress for each plate element and average these stresses according to area. This approach is conservative in most cases because of the capacity of plate elements to support load after buckling. However, the concept that the crippling stress may be obtained by averaging stresses that are characteristic of the individual elements

can still be used to formulate an empirical crippling analysis, as is illustrated in reference 3 where crippling curves are presented for plate elements of certain aluminum alloys. This concept is used in the present paper to develop crippling curves that are applicable to plate elements of any material.

For this analysis, two basic plate elements are defined: plates with one unloaded edge free (flanges) and plates with no unloaded edges free (webs). The crippling stress of any section composed of essentially flat plate elements is then given by

$$\bar{\sigma}_F = \frac{\sum A_W \bar{\sigma}_W + \sum A_F \bar{\sigma}_F}{\sum A_W + \sum A_F} \quad (2)$$

The validity of separating the crippling load into the loads carried by the individual parts, as in equation (2), is illustrated in the following sections, and appropriate expressions for $\bar{\sigma}_W$ and $\bar{\sigma}_F$ are developed.

Determination of $\bar{\sigma}_W$ and $\bar{\sigma}_F$

The basic problem is to determine expressions for $\bar{\sigma}_W$ and $\bar{\sigma}_F$ in equation (2) that will correlate with experiments conducted over a wide range of proportions and on many materials. The results of reference 4 can be used to establish a relationship between $\bar{\sigma}_W$ and b_W/t_W . In that investigation a large number of plates of various materials were tested in compression in a V-groove edge fixture in order to determine a suitable parameter to define material properties which affect plate compressive strength. From the results of these tests the parameter $(E_s \sigma_2)^{1/2}$ was found to correlate failing stresses for a variety of materials. This parameter was obtained in reference 4 from the approximate representation of the curve of average stress plotted against unit shortening for a plate after local buckling,

$$\frac{\bar{\sigma}}{\sigma_e} = \left(\frac{\epsilon_{cr}}{\epsilon_e} \right)^{1-m} \quad (3)$$

By replacing ϵ_{cr} with $K \left(\frac{t}{b} \right)^2$, the average stress corresponding to any unit shortening may be written in the form

$$\bar{\sigma} = C \frac{\sigma_e}{\epsilon_e^{1-m}} \left(\frac{t}{b} \right)^{2(1-m)} \quad (4)$$

This equation suggests that the maximum value of $\bar{\sigma}$ for a given geometry is associated with the maximum value of a quantity $\frac{\sigma_e}{\epsilon_e^{1-m}}$ evaluated from a material stress-strain curve. The maximum value of $\frac{\sigma}{\epsilon^{1-m}}$ (or its equivalent $E_s^{1-m}\sigma^m$) for any material occurs at the stress at which $E_t = (1 - m)E_s$. A general equation for crippling may then be written as

$$\bar{\sigma}_F = C \left(E_s^{1-m} \sigma^m \right)_{\max} \left(\frac{t}{b} \right)^{2(1-m)} \quad (5)$$

In reference 5 good correlation of crippling stresses for web elements was obtained in the elastic range by the use of this material parameter with m equal to $1/2$. At high stresses, where failure is influenced by plasticity, the parameter was modified by replacing the secant modulus at σ_2 with the secant modulus at the failure stress, and thus the parameter $(E_s' \sigma_2)^{1/2}$ evolved.

Representative data of reference 4 for plates tested in V-groove fixtures are shown in figure 1, where $\bar{\sigma}_W / (E_s' \sigma_2)^{1/2}$ is plotted against b_W/t_W . Also included are the crippling stresses obtained from tests of square tubes, which are in agreement with crippling stresses of plates tested in V-groove fixtures. The closeness of the points to a single curve indicates the suitability of $(E_s' \sigma_2)^{1/2}$ as a material correlation parameter. For $b_W/t_W < 45$ the test results are adequately represented by the simple equation

$$\frac{\bar{\sigma}_W}{(E_s' \sigma_2)^{1/2}} = 1.75 \frac{t_W}{b_W} \quad (6)$$

Beyond $b_W/t_W = 45$, equation (5) tends to be slightly conservative, and a value of $\bar{\sigma}_W / (E_s' \sigma_2)^{1/2}$ corresponding to the dashed curve in figure 1 should be used. The curve presented in figure 1 was also shown in reference 4 to be applicable to web elements of more complicated structures.

In the determination of an expression for $\bar{\sigma}_F$, a more indirect approach is used. If $\bar{\sigma}_W$ is assumed to be given as in figure 1, values of $\bar{\sigma}_F$ can be deduced from tests on sections containing both webs

and flanges. A large number of tests on channel and Z-sections have been made and the results are reported in references 5 to 12. The average stress carried in the flanges of these sections at maximum load is defined by equation (2) as

$$\bar{\sigma}_F = \bar{\sigma}_f + \frac{\bar{\sigma}_f - \bar{\sigma}_W}{2b_F/b_W} \quad (7)$$

From equation (7), $\bar{\sigma}_F$ was computed for the channel and Z-sections which buckled at less than three-fourths of the yield stress. The results of these calculations indicated that $\bar{\sigma}_F$ in each material was related to t_F/b_F by an equation of the form

$$\bar{\sigma}_F = K \left(\frac{t_F}{b_F} \right)^{2/3} \quad (8)$$

Comparison of equation (8) with equation (5) suggests the use of the parameter $(E_s' \sigma_3^2)^{1/3}$ to correlate flange stresses among materials.

Accordingly $\bar{\sigma}_F / (E_s' \sigma_3^2)^{1/3}$ was plotted against b_F/t_F as shown in figure 2. Deviations of the data from a single curve may be caused by (1) experimental scatter, (2) variation of the web stress from that given by figure 1, (3) variation of the flange stress due to interaction with other plate elements, and (4) the inability of simple parameters such as $(E_s' \sigma_2)^{1/2}$ and $(E_s' \sigma_3^2)^{1/3}$ to determine completely the effect of material properties on crippling. In a plot such as figure 2, errors from all sources are attributed to the flange, which represents only a portion of the total cross-sectional area; hence these deviations tend to be magnified. The low points around $b_F/t_F = 15$ correspond to tests where the length was great enough so that column action may have been present. When these factors are taken into account, the scatter is not great and on a logarithmic plot the test points tend to lie on a straight line given by the equation

$$\frac{\bar{\sigma}_F}{(E_s' \sigma_3^2)^{1/3}} = 0.65 \left(\frac{t_F}{b_F} \right)^{2/3} \quad (9)$$

where σ_3 is the stress at which $E_t = \frac{1}{3} E_s$. The line was drawn to give the best fit to the data for all the different materials.

In the preparation of figure 2, the dimensions b_F and b_W were measured between the center lines of the plate elements as indicated in the figure. The material parameters for the formed sections were calculated from an effective stress-strain curve which is described in the section entitled "Material Properties and the Effective Stress-Strain Curve." In table I are listed the values of σ_2 and σ_3 , as well as $\sigma_2/\epsilon_2^{1/2}$ and $\sigma_3/\epsilon_3^{1/3}$, which might be called the elastic values of $(E_s'\sigma_2)^{1/2}$ and $(E_s'\sigma_3)^{1/3}$. Data are given for the materials shown in figure 2 and for some materials that appear subsequently in this report.

In applying the curves of figures 1 and 2 to other sections, it was found that calculations were conservative for sections with flanges supported by more than one other plate element at a corner, such as an H-section. The higher load carried by these sections can be attributed to the increased stability of the corners when more than two plate elements support each other. By assuming that the web stresses are still given by figure 1, a new set of flange stresses can be calculated from the test results on H-sections reported in references 5 to 9. The results of these calculations, plus the crippling stress of a few cruciform sections, are shown in figure 3. An equation of the same form as equation (9) may be fitted to these data, but the coefficient is now 0.75 instead of 0.65. The assumption that the web stress is obtainable from figure 1 is strengthened by the fact that crippling stresses of cruciform sections intermingle with the flange stresses for H-sections.

An empirical equation for the average stress at failure of a flange element may then be written as

$$\frac{\bar{\sigma}_F}{(E_s'\sigma_3^2)^{1/3}} = C_F \left(\frac{t_F}{b_F} \right)^{2/3} \quad (10)$$

where C_F is 0.65 for two elements at a corner and 0.75 for more than two elements at a corner.

Alternate Form of the Crippling Equations

In reference 4 it is shown that for many materials the parameter $(E_s'\sigma_2)^{1/2}$ is approximately proportional to the parameter $(E_s\sigma_{cy})^{1/2}$, which involves commonly quoted quantities for materials. Similarly, the parameter $(E_s'\sigma_3^2)^{1/3}$ is approximately proportional to $(E_s\sigma_{cy}^2)^{1/3}$.

Although it is believed that the quantities $(E_s \sigma_2)^{1/2}$ and $(E_s \sigma_3^2)^{1/3}$ are superior to $(E_s \sigma_{cy})^{1/2}$ and $(E_s \sigma_{cy}^2)^{1/3}$ as material correlation parameters, particularly for materials having rounded stress-strain curves without a defined yield stress, the crippling equations for webs and flanges in terms of the last two parameters are often more convenient to use. The data in figures 1, 2, and 3, therefore, can also be represented by

$$\left. \begin{aligned} \bar{\sigma}_W &= 1.60 (E_s \sigma_{cy})^{1/2} \frac{t_W}{b_W} \\ \bar{\sigma}_F &= C_F (E_s \sigma_{cy}^2)^{1/3} \left(\frac{t_F}{b_F} \right)^{2/3} \end{aligned} \right\} \quad (11)$$

where C_F is 0.59 for two elements at a corner and 0.68 for more than two elements at a corner, and where E_s is associated with $\bar{\sigma}_W$ and $\bar{\sigma}_F$, respectively.

Material Properties and the Effective Stress-Strain Curve

The equations for $\bar{\sigma}_W$ and $\bar{\sigma}_F$ contain a term which represents the effect of geometry on crippling, and another term which is a measure of material properties. For sections which have uniform properties, the material parameters can be calculated directly from the compressive stress-strain curve. If a material is anisotropic or has a variation in material properties due to forming, the stress-strain curve can be modified to account for these variations. Reference 4 presents a simple empirical method of constructing this modified or effective stress-strain curve for an anisotropic material. The effective stress-strain curve was computed as a weighted average of the stress-strain curve in the loading direction and the stress-strain curve in the transverse direction, the stress-strain curve in the loading direction being weighted twice as much as the stress-strain curve in the transverse direction. The correlation that can be achieved with this type of correction is illustrated in figure 1, where test points for 18-8- $\frac{3}{4}$ H stainless steel, which is highly anisotropic, lie on the same curve as those for the isotropic materials. For most materials this correction is negligible, but it is important for a material such as 18-8- $\frac{3}{4}$ H stainless steel.

When a section is formed from flat-sheet material, the yield stress in the vicinity of formed corners is generally greater than that in the flat sheet. This increase in yield stress results in a higher crippling stress than for an identical section with uniform properties corresponding to those of the flat-sheet material. Here again it is possible to define an effective stress-strain curve which will give satisfactory correlation when used to calculate the material parameters necessary for predicting the crippling stress. Several methods of combining the properties of the formed and unformed parts of the sheet were tried, and the one that appeared to work best was also one of the simplest. It was found that the effective stress-strain curve for formed sections can be taken as the curve obtained by averaging the stress from the formed-corner stress-strain curve with the stress from the flat-sheet stress-strain curve at any given value of strain. Even though the formed material may constitute a small percentage of total area, its stress-strain curve must be weighted as heavily as that for the flat-sheet material, because crippling of a composite section is associated with failure of the corner and hence will be influenced most by the material properties in the vicinity of the formed corner. When the effective stress-strain curve is used, test points for formed sections intermingle with those for extrusions, as shown in figure 2. Although the shape of the curved corner may influence the crippling stress, the formulas imply that the effect of increased yield stress due to forming is more important. A similar observation can be made regarding the effect of the curved corner on buckling stresses. For elastic buckling the conventional formulas can be used without considering the effect of the curved corner (in general, forming does not change E); in the plastic range the formulas are conservative, a fact which may be attributed to the increase in yield stress. These conclusions are based on the tests reported in references 10 to 12, where the sections were formed to a bend radius of about three to four times the sheet thickness.

The effective stress-strain curve can also be used, in conjunction with equation (1), to calculate the buckling stress for sections of anisotropic material or for sections which have a variation in material properties due to forming. This application is illustrated in figure 4, where experimental buckling stresses from reference 10 for formed channel and Z-sections are compared with computations based on the effective stress-strain curve. The elastic buckling stress σ_{el} is computed from the conventional plate-buckling formula:

$$\sigma_{el} = \frac{k_W \pi^2 E}{12(1 - \mu^2)} \left(\frac{t_W}{b_W} \right)^2 \quad (12)$$

Values of k_W can be found in reference 13. If the effect of forming is neglected, the calculated buckling stresses are rather conservative as indicated by the lower curve in figure 4.

Therefore, the procedures and methods developed in the preceding section can be used for formed sections or anisotropic material by the introduction of the effective stress-strain curve in the calculation of buckling stresses as well as crippling stresses.

Size of Flange Necessary To Support a Web

Results of crippling tests of flanged sections show that one type of failure occurs when the flange width is large and another type when the width is small. In the first case, the joints remain straight until failure; in the second case, the flange joint is translated upon buckling and failure occurs at a reduced load. The equations developed in the preceding section apply when the flange is large; hence it is desirable to know the minimum width of flange that will force a node along a joint.

In order to establish a criterion, the flange is considered as an elastic beam providing deflectional restraint to a web. From the solution for the buckling stress of a plate restrained by elastic beams, the significant parameters defining the restraint offered by the flange may be determined. In this solution, given by Timoshenko in reference 14, it is seen that the buckling stress is a function of a stiffness parameter θ . For a flange supporting a web,

$$\theta = \frac{EI_F}{b_W D_W} - \frac{A_F \sigma_{cr} a^2}{b_W D_W^2 \pi^2} \quad (13)$$

and as θ approaches infinity the buckling stress approaches that of a simply supported plate. For the proportions encountered in most sections, the significant quantity in equation (13) was found to be $EI_F/b_W D_W$,

which may be written as $K(b_F/b_W)^3(b_W/t_W)^2(t_F/t_W)$. By computing the crippling stresses of sections with relatively small flanges, it was found that if the quantity $(b_F/b_W)^3(b_W/t_W)^2(t_F/t_W)$ was greater than 20 the calculations were generally in agreement with tests, but if this quantity was less than 20 the predictions were often unconservative.

Most flange proportions encountered in practice are more than adequate to support the webs effectively. In some cases, however, sections such as hat or Z-sections may have an additional small flange or lip which is not large enough to satisfy the criterion. In figure 5 the crippling stresses on lipped Z-sections are plotted against the size of the lip. When the width of the lip is large, corresponding to

$$\left(\frac{b_F}{b_W}\right)^3 \left(\frac{b_W}{t_W}\right)^2 \left(\frac{t_F}{t_W}\right) > 20 \quad (14)$$

$\bar{\sigma}_F$ can be predicted by the method of the present investigation. Also, when the lip width is zero, $\bar{\sigma}_F$ can be computed as for a plain Z-section. The intermediate test points can be adequately predicted by drawing a straight line from the value of $\bar{\sigma}_F$ corresponding to the smallest value of b_F/b_W that will satisfy relationship (14) to the value of $\bar{\sigma}_F$ representing the crippling stress of a plain Z-section.

EXPERIMENTAL VERIFICATION

The method developed in the previous sections is based primarily on tests of aluminum-alloy channel and Z-sections. The applicability of the procedure to other shapes, other materials, sections tested at elevated temperature, and sections which have been fabricated with riveted joints is illustrated in the following paragraphs.

Arbitrary Cross Section

In connection with the analysis of reference 2, a group of 24S-T3 (now called 2024-T3) clad aluminum-alloy sections were tested. These sections were formed to give many different combinations of webs and flanges such as lipped-angle, channel, and Z-sections, hat sections, and various other shapes. In table II, predictions of crippling stresses based on the method developed herein are compared with the test data reported in table VI of reference 2. Calculations are based on the material properties given in table IV of reference 2, and agreement is seen to be satisfactory.

Other Materials

The stress-strain curve of stainless steel is substantially different from that of the aluminum alloys in both height and shape. Because of these differences a few tests on channel and hat sections of stainless steel were made to substantiate the applicability of the method to other materials. Test results along with predictions are shown in table III. It should be noted that there is a marked increase in yield stress due to forming of the corners, as well as a considerable difference between the with-grain and cross-grain properties. Predictions based on the effective stress-strain curve, which weights these variations in yield stress, are within about ± 7 percent of the test results except for one test for which the prediction was conservative by about 12 percent.

Elevated Temperatures

Inasmuch as the crippling stress is given as a function of material properties calculated from the stress-strain curve, it is expected that the equation will apply to tests at elevated temperature if the appropriate elevated-temperature stress-strain curve is used. The correlation that can be achieved is illustrated in figure 6, where predictions are compared with the experimental crippling stresses of H-sections tested at elevated temperatures and reported in reference 15. Predictions are conservative for low values of b_W/t_W .

Fabricated Sections

An important application of a crippling analysis is the calculation of the crippling strength of fabricated structures such as sheet-stringer panels. However, the behavior of these panels may be affected greatly by the design of the riveted attachment flange between sheet and stringer, as shown in reference 16. The crippling curves presented herein may be expected to apply when near-integral attachment of the sheet to the stringer is achieved by the riveted joints. To check the accuracy of the procedure, the crippling stresses of the panels reported on in reference 17 were calculated and are compared with experiment in table IV. These panels had extruded Y-section stiffeners and, according to the results of reference 16, the rivet attachment was sufficient to achieve near-integral behavior. The experimental crippling stresses are for panels having slenderness ratios of 20 or 40. The material properties of the 7075-T6 aluminum alloy varied enough from the average so that as much as 7 percent scatter could be expected for this reason alone. In most cases the scatter is less than 7 percent, but in a few cases it is as high as 11 percent. The overall correlation appears to be satisfactory.

DISCUSSION

The empirical crippling-strength equations presented give the average stress carried by each of the individual plate elements which comprise a structural section. The loads carried by each element may be obtained by multiplying equations (6) and (10) by the appropriate area to give

$$\frac{P}{t_W^2} = 1.75 (E_S \sigma_2)^{1/2} \quad (15)$$

for a web with $b_W/t_W < 45$, and

$$\frac{P_F}{t_F^2} = C_F (E_S \sigma_2^2)^{1/3} \left(\frac{b_F}{t_F} \right)^{1/3} \quad (16)$$

for a flange. It is seen that, for a given thickness, the load carried by a web of the width-thickness ratios encountered in stiffeners is constant except when b_W/t_W is small enough so that the crippling stress is in the plastic range, whereas a flange will support a load that increases with b_F/t_F . From equations (15) and (16), the distribution of material which gives the highest crippling stress can be quickly determined. For example, in a channel or Z-section, the optimum proportion will be such that $\bar{\sigma}_W$ is close to σ_2 , inasmuch as at this value of stress an increase in web width will not increase the web load. Calculations by the present method indicate that $\bar{\sigma}_F$ for a channel or Z-section may be reduced as much as 10 or 15 percent if the distribution of material between the flange and web is not optimum. Some investigations, such as those of references 2 and 12, have ignored the effect of distribution of material and have presented crippling equations for channel and Z-sections that give $\bar{\sigma}_F$ as a function of b'/t ($b' = b_W + 2b_F$, the developed width of the section). In other words, if a channel or Z-section is formed from a sheet of a certain width, these formulas give the same crippling stress for any ratio of b_F/b_W .

In order to show experimentally the effect of distribution of material, the crippling results for the channel sections tested in reference 10 have been plotted in figure 7. Values of $\bar{\sigma}_F$ are plotted against b_F/b_W for constant values of b'/t by cross-plotting the data given in figure 21 of reference 10. Assuming that $\bar{\sigma}_F$ is a function of b'/t alone will in some cases lead to appreciable error. In order to study further the effect of material distribution on the strength of sections, a series of 7075-T6 Z-sections with essentially constant values of b'/t were tested. These results are listed in table V and plotted in figure 8. Buckling stresses were computed from equation (12) directly, as $\eta = 1$ in all cases. A variation in $\bar{\sigma}_F$ is apparent (about 10 percent) and the method of the present paper adequately predicts the crippling stress throughout the range of proportions.

As stated previously, the value of b_F/b_W at which $\bar{\sigma}_F$ is a maximum for a channel or Z-section will be such that $\bar{\sigma}_W$ approximately equals σ_2 . For the Z-sections of figure 8, where $b'/t = 60$, this condition will occur at $b_F/b_W \approx 0.9$. However, the maximum value of the buckling stress is at $b_F/b_W \approx 0.4$, which means that for a certain range $\bar{\sigma}_F$ was increasing while σ_{cr} was decreasing. In other words, if a section is so proportioned as to maximize the buckling stress, the proportions will not necessarily be optimum for crippling.

Earlier investigators discovered an apparent discrepancy between crippling tests of formed and extruded sections that could not be readily explained. When $\bar{\sigma}_f$ was plotted against σ_{cr} , one curve resulted for extrusions, whereas a family of curves applied to formed sections. (See, for example, fig. 12 of ref. 1.) The difference was thought to be caused by the presence of the curved corner and the increase in yield stress due to forming, but it was not accounted for quantitatively. These conclusions, however, were drawn from tests on extrusions with $b_W/t_W < 25$. In this range of proportions, a critical examination of the data shows that extrusions and formed sections have essentially the same behavior; that is, crippling results tend to lie on one curve when $\bar{\sigma}_f$ is plotted against σ_{cr} . It could be expected, then, that if information were made available for extrusions with $b_W/t_W > 25$ a family of curves of $\bar{\sigma}_f$ against σ_{cr} could be plotted. Accordingly, as part of the present investigation, tests were made of extruded Z-sections with b_W/t_W equal to 30, 35, and 40. The failing stresses, which are given in table VI, are seen to be definitely lower than the predictions of reference 2 but are in agreement with the method of the present paper. Since each shape and proportion has a separate relationship of σ_{cr} to $\bar{\sigma}_f$, the crippling stress of a structure cannot in general be predicted by using an empirical relationship between σ_{cr} and $\bar{\sigma}_f$ found for another shape or proportion.

Although the equations developed herein are based on tests where buckling occurred at less than three-fourths of the yield stress, it was found that in many cases they could be extended through the entire stress range without serious loss in accuracy. In general, if the section is predominantly composed of webs or if the flanges are supported by more than one other element at a corner, the procedure will yield satisfactory results throughout the range of stress. Calculated results appearing in figures 6 and 7 in many cases involve stresses which are much greater than three-fourths of the yield stress and yet are in good agreement with experiment. The method was noted to be as much as 15 percent conservative in the plastic range when the area of the flanges was a significant portion of the total area, as in a channel or Z-section. Inasmuch as the plastic buckling stress cannot always be easily computed, the method presented herein is recommended for all cases, but the crippling stress should never be taken lower than the plastic buckling stress if it is known.

CONCLUSIONS

An empirical analysis of the crippling strength of structural sections has been presented. The method applies to both extruded and

formed sections of arbitrary shape and proportion. The following conclusions can be drawn from the analysis.

1. To satisfy the purpose of a strength analysis, the crippling load for an integral cross section may be taken as the sum of a set of defined crippling loads which are characteristic of the individual plate elements.

2. The load carried by a plate element of any material is proportional to a parameter which can be easily calculated from the compressive stress-strain curve.

3. The presence of formed or anisotropic material can be accounted for by using an effective stress-strain curve in calculating the material parameters.

4. A simple criterion defines the minimum size of flange necessary to maintain nodes at a joint after buckling. For sections with flanges smaller than this minimum size, an extension of the basic procedure can be used to calculate the crippling stress.

5. Proportioning a section to maximize the buckling stress will not necessarily maximize the crippling stress.

Langley Aeronautical Laboratory,
National Advisory Committee for Aeronautics,
Langley Field, Va., September 12, 1955.

REFERENCES

1. Schuette, E. H.: Observations on the Maximum Average Stress of Flat Plates Buckled in Edge Compression. NACA TN 1625, 1949.
2. Needham, Robert A.: The Ultimate Strength of Aluminum-Alloy Formed Structural Shapes in Compression. Jour. Aero. Sci., vol. 21, no. 4, Apr. 1954, pp. 217-229.
3. Crockett, Harold B.: Predicting Stiffener and Stiffened Panel Crippling Stresses. Jour. Aero. Sci., vol. 9, no. 13, Nov. 1942, pp. 501-509.
4. Anderson, Roger A., and Anderson, Melvin S.: Correlation of Crippling Strength of Plate Structures With Material Properties. NACA TN 3600, 1955.
5. Heimerl, George J., and Roy, J. Albert: Column and Plate Compressive Strengths of Aircraft Structural Materials - Extruded 75S-T Aluminum Alloy. NACA WR L-173, 1945. (Formerly NACA ARR L5F08a.)
6. Heimerl, George J., and Roy, J. Albert: Column and Plate Compressive Strengths of Aircraft Structural Materials - Extruded 24S-T Aluminum Alloy. NACA WR L-32, 1945. (Formerly NACA ARR L5F08b.)
7. Heimerl, George J., and Fay, Douglas P.: Column and Plate Compressive Strengths of Aircraft Structural Materials - Extruded R303-T Aluminum Alloy. NACA WR L-33, 1945. (Formerly NACA ARR L5H04.)
8. Heimerl, George J., and Niles, Donald E.: Column and Plate Compressive Strengths of Aircraft Structural Materials - Extruded 14S-T Aluminum Alloy. NACA WR L-284, 1946. (Formerly NACA ARR L6C19.)
9. Heimerl, George J., and Niles, Donald E.: Column and Plate Compressive Strengths of Aircraft Structural Materials - Extruded O-1HTA Magnesium Alloy. NACA TN 1156, 1947.
10. Lundquist, Eugene E., Schuette, Evan H., Heimerl, George J., and Roy, J. Albert: Column and Plate Compressive Strengths of Aircraft Structural Materials - 24S-T Aluminum-Alloy Sheet. NACA WR L-190, 1945. (Formerly NACA ARR L5F01.)

11. Heimerl, George J., and Roy, J. Albert: Column and Plate Compressive Strengths of Aircraft Structural Materials - 17S-T Aluminum-Alloy Sheet. NACA WR L-20, 1945. (Formerly NACA ARR L5F08.)
12. Gallaher, George L.: Plate Compressive Strength of FS-1h Magnesium-Alloy Sheet and a Maximum-Strength Formula for Magnesium-Alloy and Aluminum-Alloy Formed Sections. NACA TN 1714, 1948.
13. Kroll, W. D., Fisher, Gordon P., and Heimerl, George J.: Charts for Calculation of the Critical Stress for Local Instability of Columns With I-, Z-, Channel, and Rectangular-Tube Section. NACA WR L-429, 1943. (Formerly NACA ARR 3K04.)
14. Timoshenko, S.: Theory of Elastic Stability. McGraw-Hill Book Co., Inc., 1936, pp. 345-349.
15. Heimerl, George J., and Roberts, William M.: Determination of Plate Compressive Strengths at Elevated Temperatures. NACA Rep. 960, 1950. (Supersedes NACA TN 1806.)
16. Semonian, Joseph W., and Peterson, James P.: An Analysis of the Stability and Ultimate Compressive Strength of Short Sheet-Stringer Panels With Special Reference to the Influence of Riveted Connection Between Sheet and Stringer. NACA TN 3431, 1955.
17. Dow, Norris F., and Hickman, William A.: Design Charts for Flat Compression Panels Having Longitudinal Extruded Y-Section Stiffeners and Comparison With Panels Having Formed Z-Section Stiffeners. NACA TN 1389, 1947.



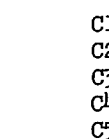
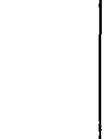
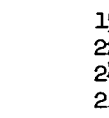
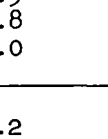

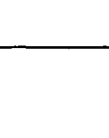
TABLE I
VALUES OF MATERIAL PARAMETERS

Material ^a		σ_2 ,	$\sigma_2/\epsilon_2^{1/2}$,	σ_3 ,	$\sigma_3/\epsilon_3^{1/3}$,
Old designation	New designation	ksi	ksi	ksi	ksi
Extruded	75S-T6	73	854	75	378
	R303-T	68	819	70	359
	14S-T6	58	757	60	324
	24S-T4	45	659	48	272
	0-1HTA (Magnesium)	31	425	32	180
Formed ^b	24S-T3	46	624	56	273
	17S-T	43	596	49	254
	FS-1h (Magnesium)	26	372	27	153
	24S-T3 clad	44	615	50	262
	18-8 - $\frac{3}{4}$ H (Stainless steel)	154	1,770	175	812
	75S-T6	70	843	72	377

^aAluminum alloy unless otherwise indicated.

^bProperties for formed sections were obtained from effective stress-strain curves.

TABLE II
 COMPARISON OF EXPERIMENTAL AND PREDICTED CRIPPLING STRESSES
 FOR FORMED 2024-T3 CLAD SECTIONS

Cross section	Specimen	$\bar{\sigma}_f$, ksi	
		Experimental ^a	Predicted ^b
	A1	26.2	26.6
	A2	22.9	23.4
	B1	20.8	22.6
	B2	27.1	28.4
	C1	17.3	15.8
	C2	24.1	24.0
	C3	27.5	28.4
	C4	31.4	33.9
	C5	24.0	23.8
	D1	17.4	16.3
	D2	28.2	28.5
	D3	23.3	23.9
	D4	19.0	19.8
	D5	27.7	29.2
	E1	15.8	15.0
	E2	22.6	22.3
	E3	24.7	25.8
	E4	21.0	20.8
	F1	23.9	23.6
	F2	23.8	24.4
	F3	35.0	36.9
	G1	26.2	25.4
	G2	17.8	17.2
	H	25.0	26.0

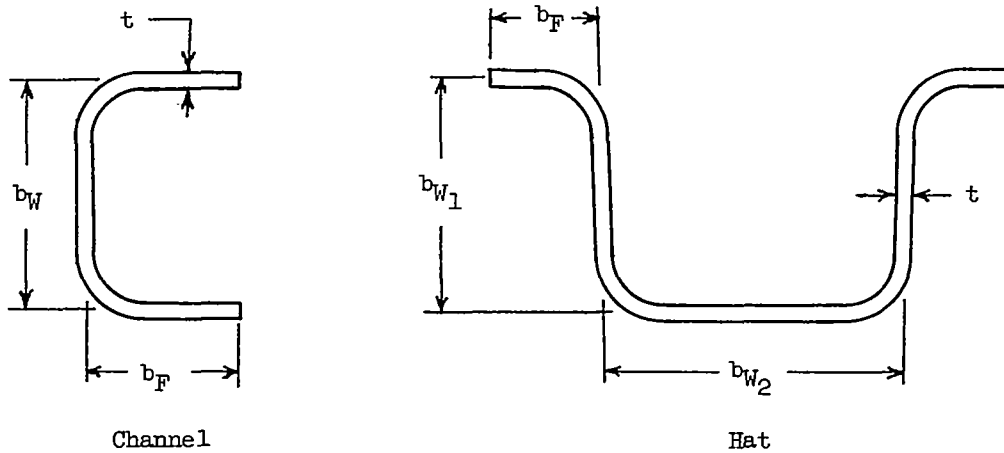
^aFrom table VI of reference 2.

^bBased on the material properties in table IV of reference 2.

TABLE III

CRIPPLING STRESS OF 18-8- $\frac{3}{4}$ H STAINLESS-STEEL SECTIONS

$E = 29,000 \text{ ksi}; \sigma_{cy} \text{ (with grain)} = 111 \text{ ksi};$
 $\sigma_{cy} \text{ (cross grain)} = 170 \text{ ksi}; \sigma_{cy} \text{ (formed corner)} = 166 \text{ ksi}$



Channel Sections

$\frac{b_W}{t}$	$\frac{b_F}{b_W}$	$\bar{\sigma}_F, \text{ ksi}$	
		Experimental	Predicted
30.6	0.352	120	105
29.7	.515	97.4	95.1
30.2	.652	82.1	85.5
30.6	.835	73.2	76.0
30.4	1.00	68.5	70.4
30.3	1.33	57.0	60.6

Hat Sections

$\frac{b_{W1}}{t}$	$\frac{b_{W2}}{t}$	$\frac{b_F}{t}$	$\bar{\sigma}_F, \text{ ksi}$	
			Experimental	Predicted
20.1	24.6	15.8	133	123
30.0	35.4	15.3	95.8	94.6
40.6	48.5	15.7	70.0	74.0
50.3	60.5	15.2	59.4	62.2

TABLE IV
 COMPARISON OF EXPERIMENTAL AND PREDICTED CRIPPLING STRESSES
 FOR PANELS WITH EXTRUDED Y-SECTION STIFFENERS

$\frac{b_S}{t_S}$	$\frac{b_W}{t_W}$	$\frac{t_W}{t_S}$	$\bar{\sigma}_F$, ksi, for 2024-T		$\bar{\sigma}_F$, ksi, for 7075-T6	
			Experimental ^a	Predicted	Experimental ^a	Predicted
25	20	0.40	42.7	43.2	58.1	57.0
35	20	.40	36.9	37.0	52.3	53.2
50	20	.40	32.0	30.8	43.9	43.7
25	25	.40	43.0	43.0	58.2	61.8
35	25	.40	36.0	37.3	49.1	53.0
50	25	.40	31.4	31.4	43.6	44.0
25	30	.40	43.3	42.0	----	----
35	30	.40	36.2	37.1	47.4	52.8
50	30	.40	30.6	31.5	----	----
25	20	.63	45.1	43.3	63.3	66.9
35	20	.63	40.6	39.2	54.7	59.7
50	20	.63	34.6	34.6	51.0	52.1
75	20	.63	30.0	29.1	43.5	43.9
25	25	.63	41.5	42.0	58.9	63.1
35	25	.63	37.4	38.4	55.1	57.3
50	25	.63	34.8	34.3	51.2	50.5
75	25	.63	30.1	29.4	43.8	43.4
25	30	.63	41.0	40.2	----	----
35	30	.63	36.8	37.2	49.9	55.1
45	30	.63	33.6	33.5	46.6	48.9
75	30	.63	30.6	29.1	39.7	42.7
25	20	1.00	42.4	42.3	64.0	67.1
35	20	1.00	41.1	40.2	58.3	63.3
45	20	1.00	38.7	37.2	57.0	58.5
75	20	1.00	34.2	33.4	49.6	52.3
25	25	1.00	39.1	40.3	58.7	61.4
35	25	1.00	39.1	38.5	54.8	58.0
45	25	1.00	37.0	36.2	53.1	54.4
75	25	1.00	34.2	32.9	47.7	49.5
35	30	1.00	37.6	36.5	48.3	53.2
45	30	1.00	35.3	34.7	47.1	52.0
75	30	1.00	31.7	31.8	43.5	48.0

^aFrom reference 17.

TABLE V
 DIMENSIONS AND TEST RESULTS FOR FORMED 7075-T6
 ALUMINUM-ALLOY Z-SECTIONS^a

$$[E = 10,500 \text{ ksi}; \sigma_{cy} = 72.5 \text{ ksi}]$$

b_W/t_W	b_F/b_W	a/b_W	Area, sq in.	σ_{cr} , ksi	$\bar{\sigma}_F$, ksi
41.7	0.214	2.55	0.593	27.0	41.0
29.9	.491	4.82	.594	34.6	43.5
30.1	.490	4.82	.595	29.4	43.1
21.6	.870	6.27	.595	22.4	45.0
22.0	.863	6.21	.590	21.2	44.9
15.2	1.46	8.89	.599	20.2	41.6
14.7	1.51	9.11	.600	19.0	41.5

^aThickness of sheet was nominally 0.102 inch with $b'/t = 60$.

TABLE VI
 CRIPPLING STRESS OF EXTRUDED 7075-T6 ALUMINUM-ALLOY
 Z-SECTIONS WITH $b_W/t_W > 25$

$$[\sigma_{cy} = 78.6 \text{ ksi}; E = 10,500 \text{ ksi}]$$

b_W/t_W	σ_{cr} , ksi	Experimental $\bar{\sigma}_F$, ksi	Predicted $\bar{\sigma}_F$, ksi	
			Present investigation	Reference 1 ^a
30.4	39.2	47.1	47.6	52.8
50.2	39.4	47.3	47.8	53.0
30.4	39.3	47.0	47.6	52.9
35.4	25.5	40.3	42.7	47.4
35.4	26.5	41.4	44.0	47.9
41.0	24.4	37.2	38.7	46.8
39.8	23.8	38.5	39.4	46.6
39.5	25.1	38.9	39.7	47.2

$$^a \bar{\sigma}_F = 0.80 \sigma_{cr}^{1/4} \sigma_{cy}^{3/4}$$

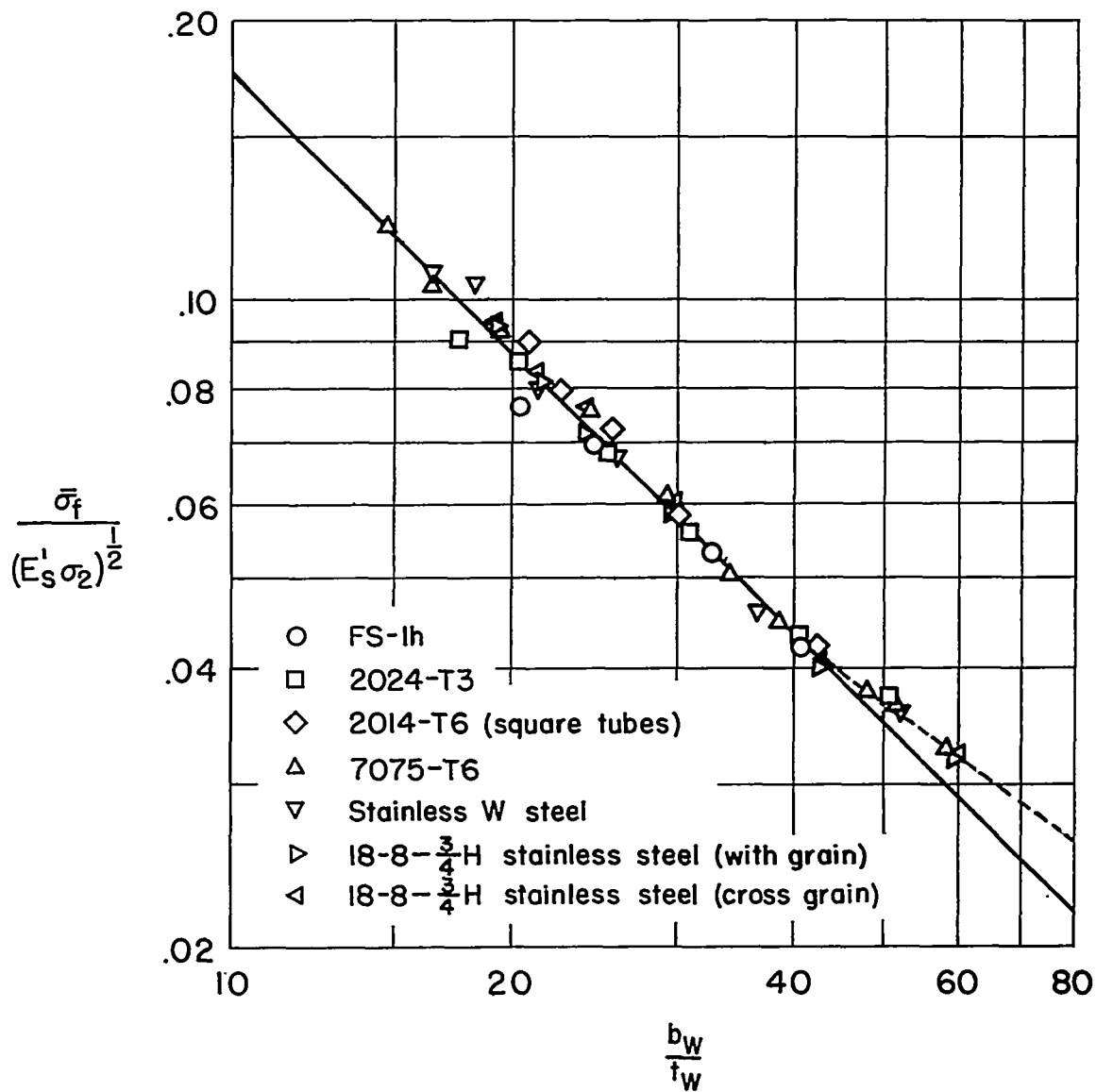


Figure 1.- Correlation of maximum average stress with material properties for plates (ref. 4).

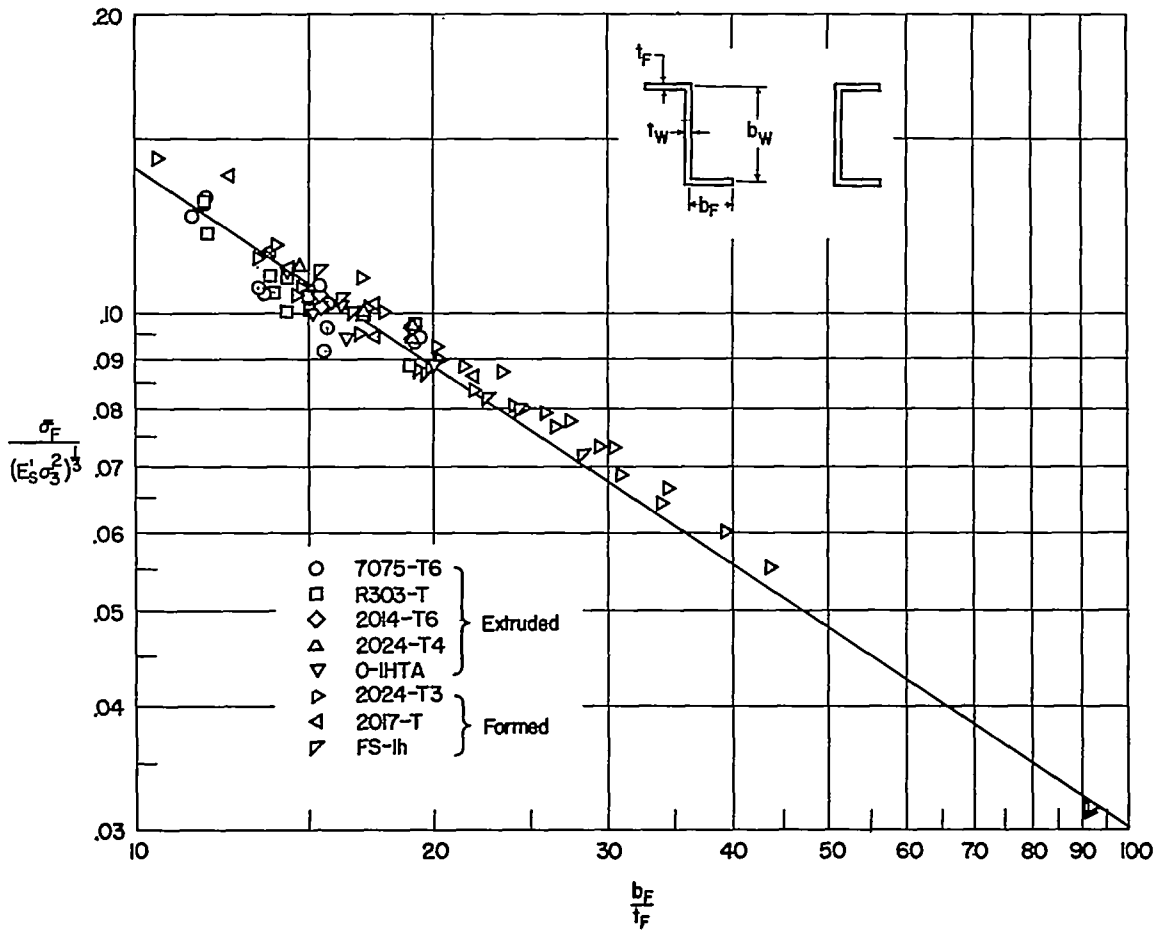


Figure 2.- Correlation of maximum average stress with material properties for flanges of channel and Z-sections. (Points at $b_F/t_F \approx 90$ are from unpublished data; other points are from refs. 5 to 12.)

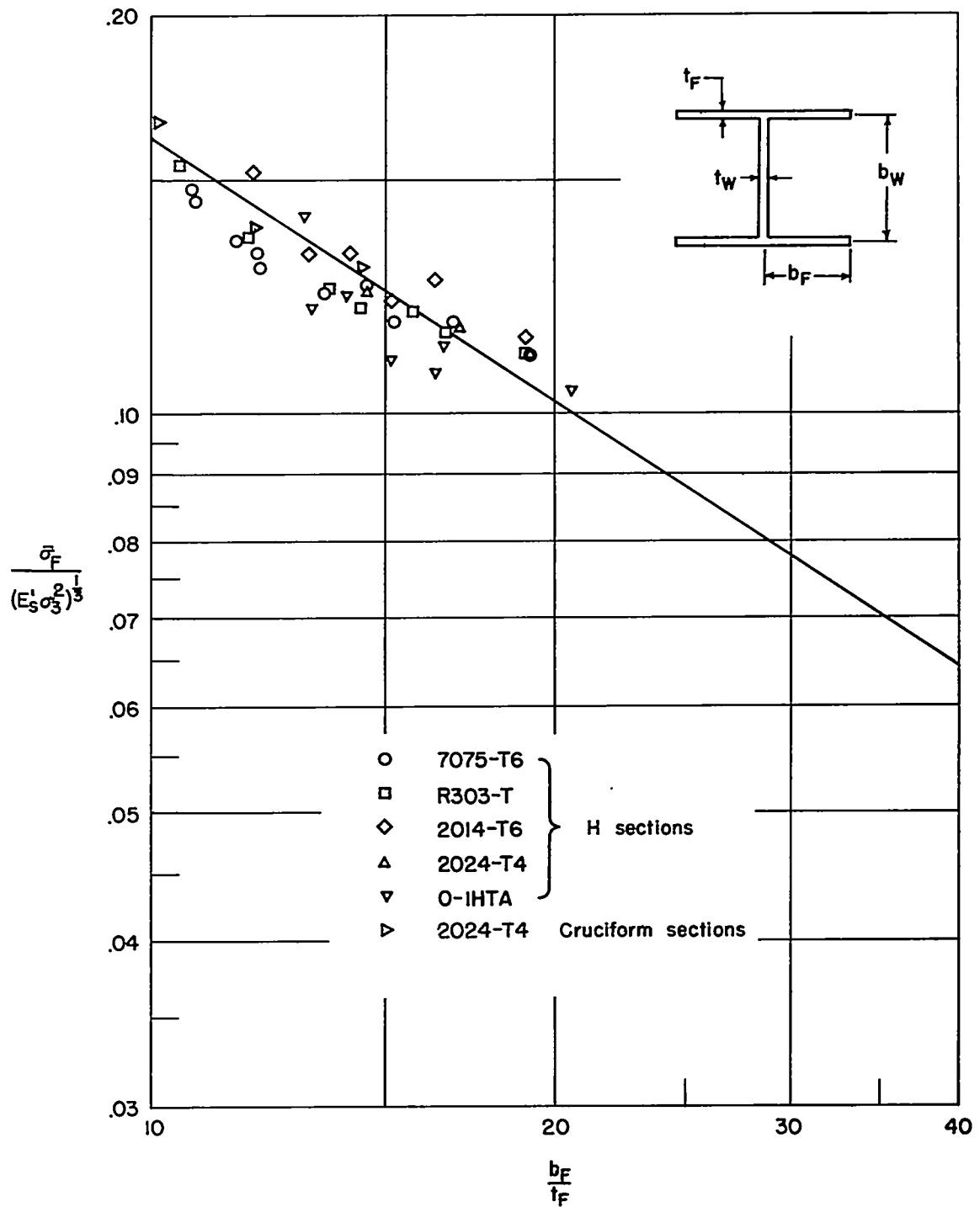


Figure 3.- Correlation of maximum average stress with material properties for flanges of H-sections. (Points for cruciform sections are from unpublished data; other points are from refs. 5 to 9.)

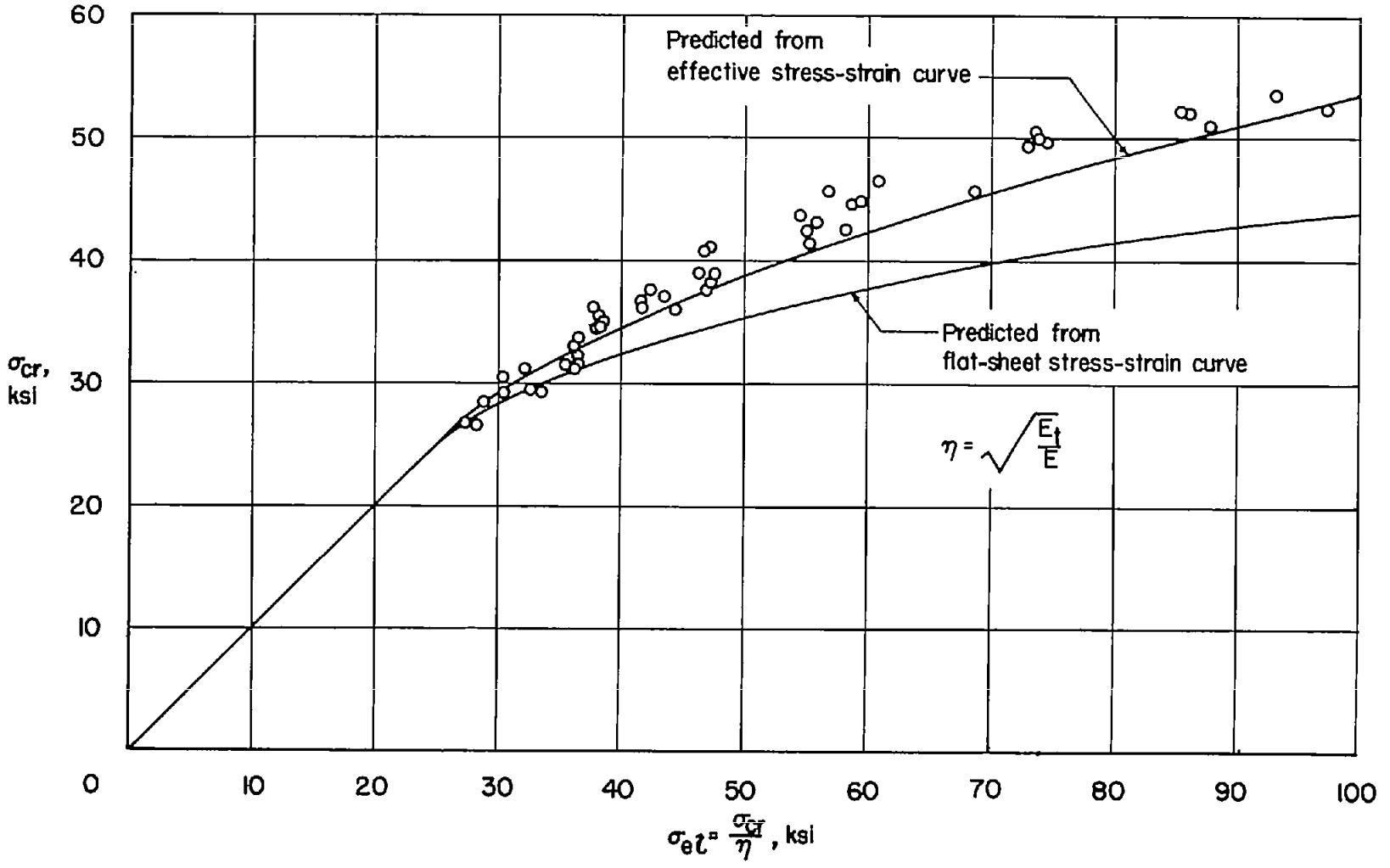


Figure 4.- Buckling stress of 2024-T3 aluminum-alloy channel and Z-sections (ref. 10).

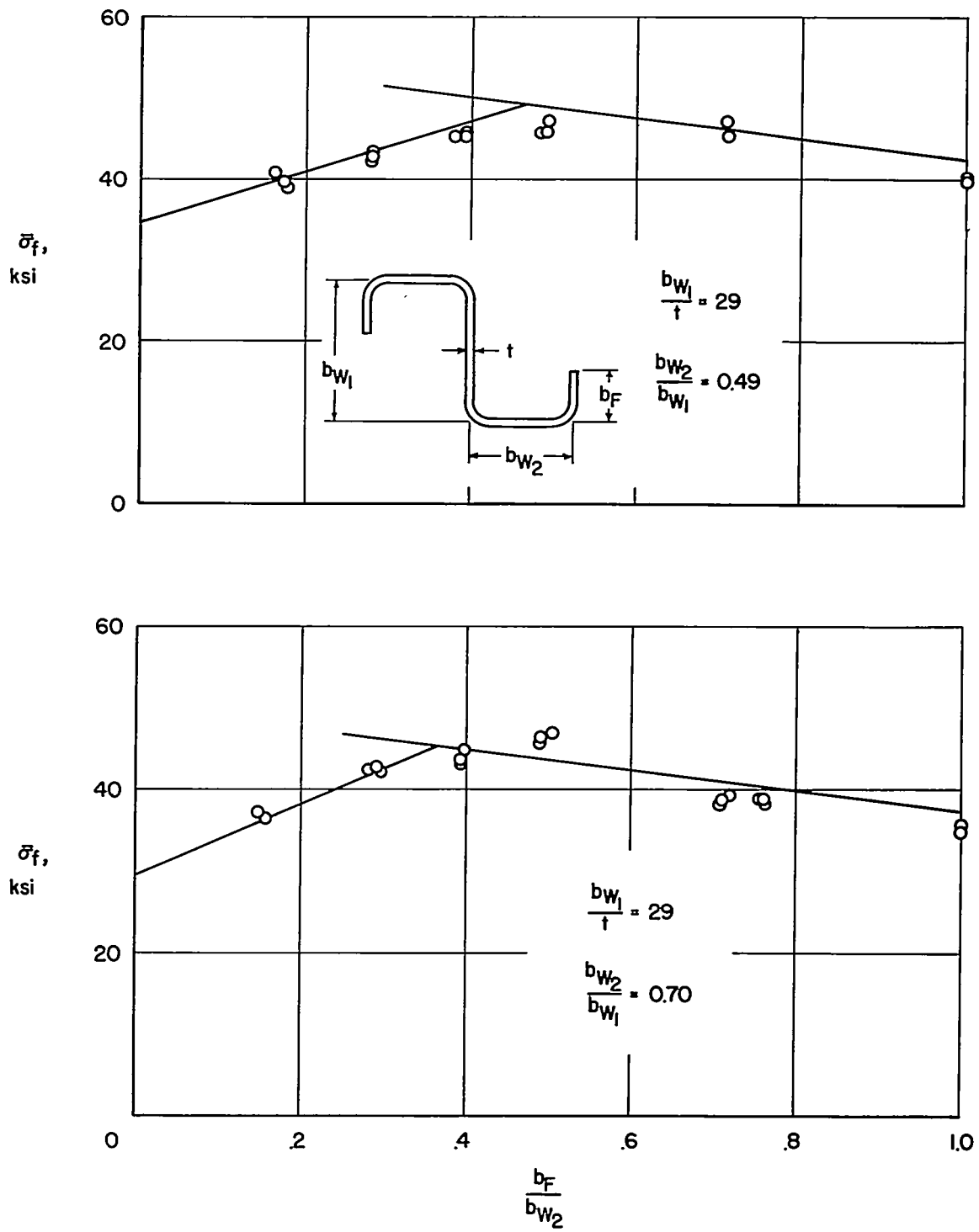


Figure 5.- Comparison of predicted and experimental crippling stresses for 2024-T3 aluminum-alloy lipped Z-sections.

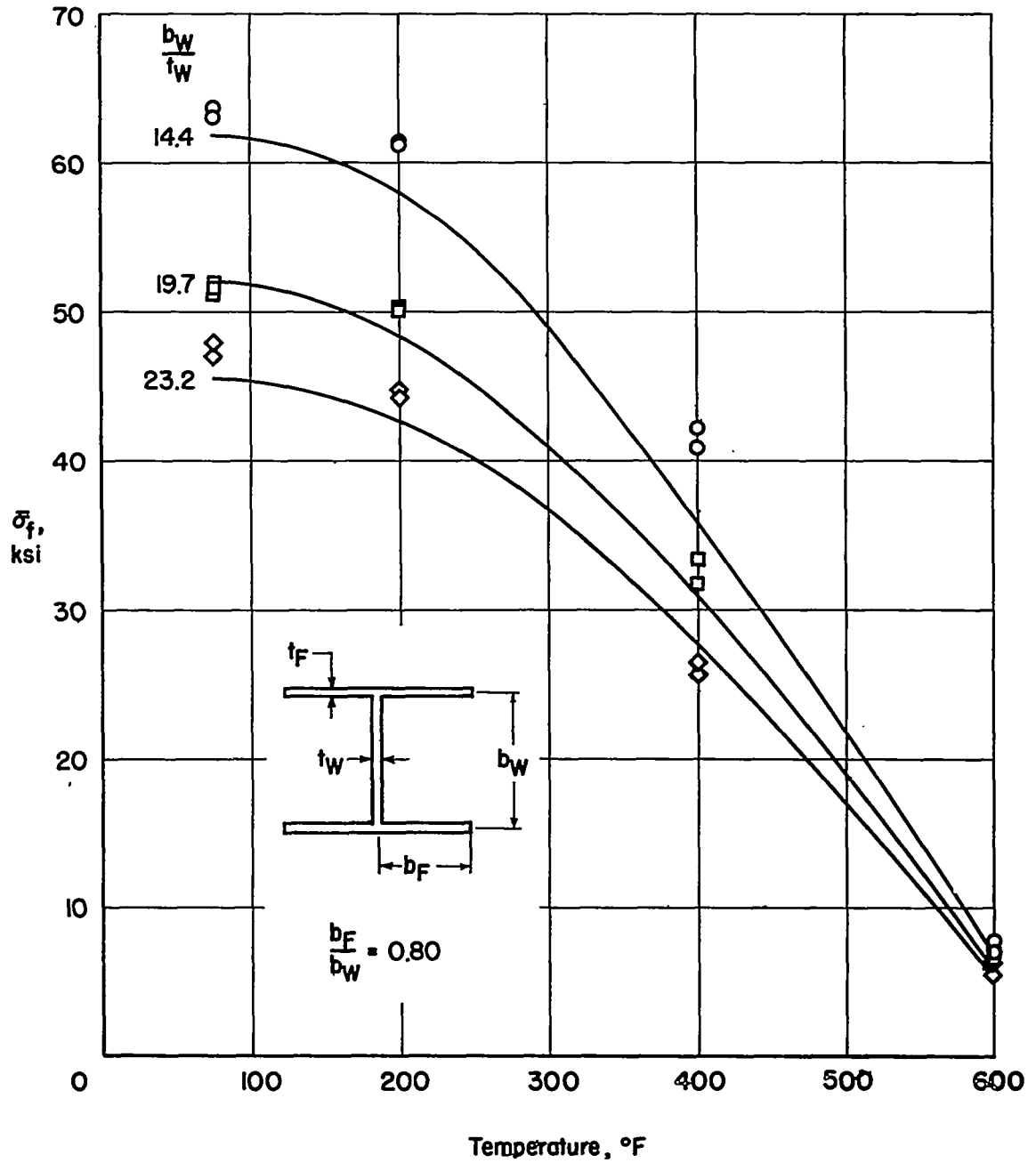


Figure 6.- Comparison of predicted and experimental crippling stresses for 7075-T6 aluminum-alloy H-sections at elevated temperatures. (Points at room temperature are from ref. 5; other points are from ref. 15.)

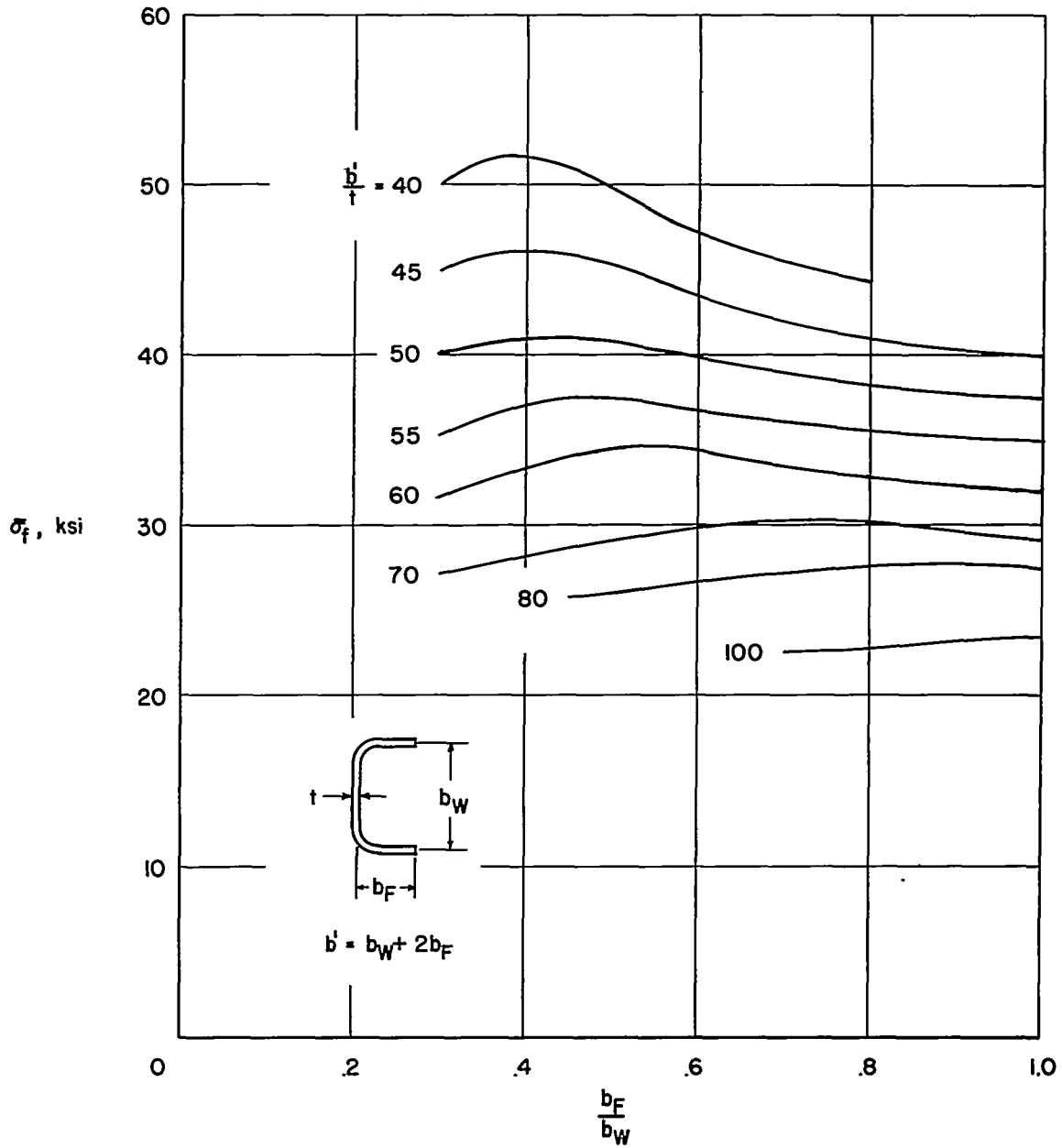


Figure 7.- Experimental crippling stress of 2024-T3 aluminum-alloy channel sections (ref. 10).

NACA - Langley Field, Va.

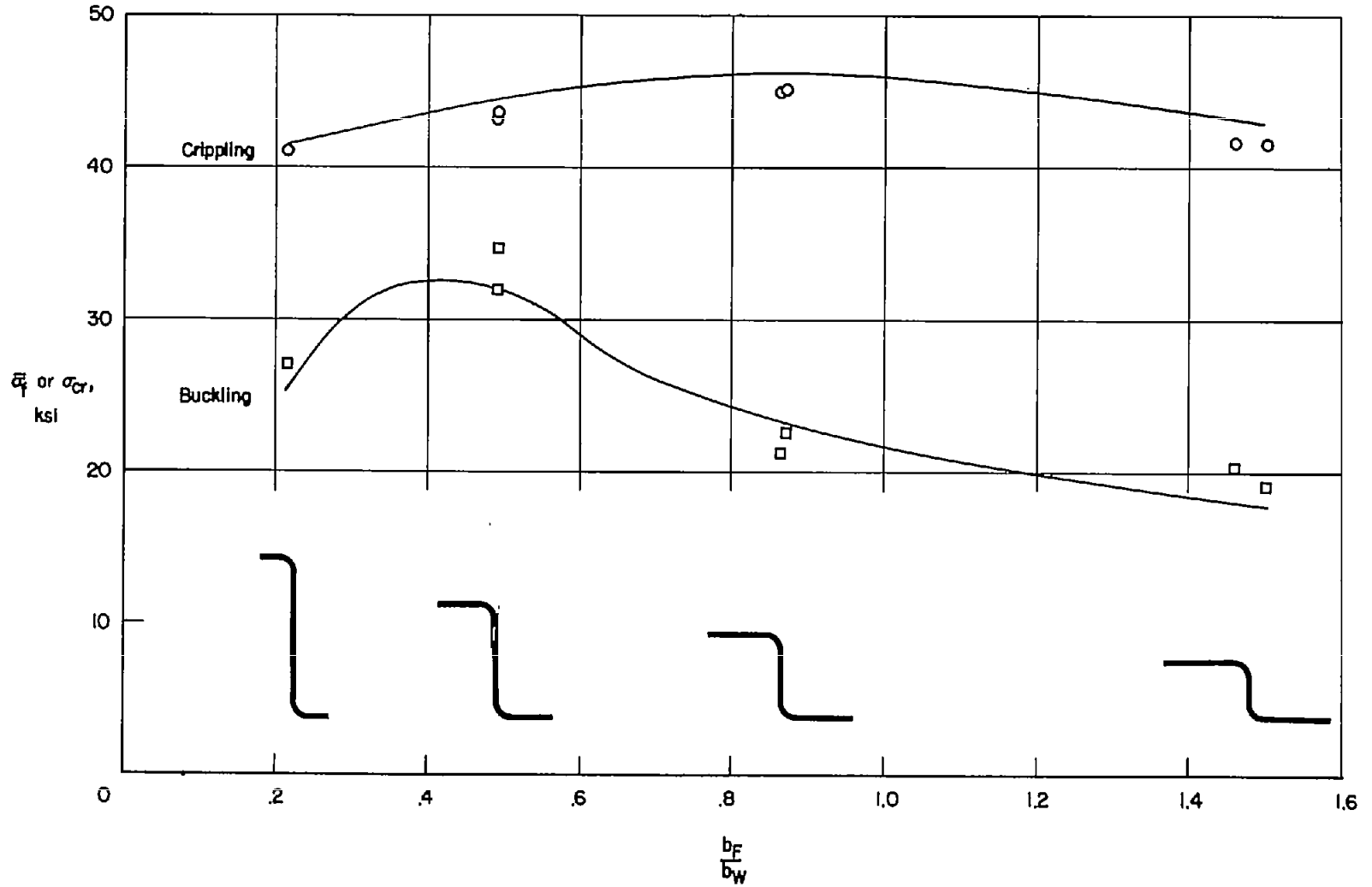


Figure 8.- Comparison of predicted and experimental buckling and crippling stresses of 7075-T6 aluminum-alloy Z-sections. $b'/t = 60$.